

of PtCl_6^{2-} (eq 1) in terms of an excited state with a subpicosecond lifetime, not observed in this work, forming PtCl_5^{2-} with a 210-ps lifetime. The latter is anticipated intuitively on the basis of the homolytic bond cleavage action. Presumably the decay of the PtCl_5^{2-} represents its solvation or aquation leading to the formation of the longer lived and less strongly absorbing platinum(III) aquo species, and the presence of some residual absorption is suggestive of this.

Acknowledgment. The support of the Natural Sciences and Engineering Research Council of Canada and the North Atlantic Treaty Organization and the assistance of Dr. S. H. Lee in performing the fluorometry measurements are very much appreciated. The calculations have been performed at the CNRS Centre at Montpellier.

Registry No. PtCl_6^{2-} , 16871-54-8; PtCl_5^{2-} , 34076-49-8.

Contribution from the Department of Chemistry,
Princeton University, Princeton, New Jersey 08544

Resonance Raman Spectra of the Ground and Charge-Transfer Excited State of Pentaammine(4,4'-bipyridine)ruthenium(II) and Pentaammine(4,4'-bipyridinium)ruthenium(II)

D. S. Caswell and T. G. Spiro*

Received March 17, 1986

Resonance Raman (RR) spectra are reported for aqueous $\text{Ru}^{\text{II}}(\text{NH}_3)_5(4,4'\text{-bipyridine})$ (I) and $\text{Ru}^{\text{II}}(\text{NH}_3)_5(4,4'\text{-bipyridine-H}^+)$ (IH^+) in resonance with their charge-transfer absorptions (480 and 570 nm) using CW (Kr^+ , 530.9 nm) and pulsed (YAG, 532 nm) laser excitation. Several RR bands are observed, which are assignable to symmetric and antisymmetric combinations of pyridine ring modes by comparison with the biphenyl vibrational spectrum. The previously reported RR spectra of $\text{Ru}(2,2'\text{-bipyridine})_3^{2+}$ and of its charge-transfer excited state are also assigned in this framework. At high pulsed laser power levels new Raman bands grow in, which are attributed to ring modes in the charge-transfer excited states by analogy with the biphenyl radical anion RR spectrum. Even though the lifetimes of the charge-transfer states are known from transient absorption spectroscopy to be 36 and 230 ps for I and 30 ps for IH^+ , the photon flux is estimated to be sufficient to produce a detectable steady-state population of excited molecules. The excited-state RR spectrum for I at pH 7 appears to contain overlapping contributions from protonated and unprotonated molecules. Although this behavior is not unexpected in view of the enhanced basicity anticipated for the uncoordinated pyridine N atom in the charge-transfer state, for which a pK_a of 11.4 is estimated, the short excited-state lifetimes imply that protonation must occur more rapidly than the equilibrium rate.

Introduction

Ruthenium(II) complexes of nitrogen heterocycles have attracted much interest because of the rich photophysical and photochemical phenomena associated with the $\text{Ru} \rightarrow$ heterocycle charge-transfer interactions. $\text{Ru}(\text{bpy})_3^{2+}$ ($\text{bpy} = 2,2'\text{-bipyridine}$) has been especially popular as a photoelectron-transfer agent because of its strong charge-transfer absorption in the visible region and the relatively long life of its charge-transfer excited state.¹⁻⁴ The nature of this state has been probed extensively, and has recently been determined, via analysis of its resonance Raman (RR) spectrum by Woodruff and co-workers^{5,6} and by Forster and Hester,⁷ to involve localization of charge on one of the bipyridine ligands. Localization has also been explored in mixed-ligand complexes involving 2,2'-bipyridine.⁸⁻¹⁰

In pentaammineruthenium(II) heterocycle complexes, the energy of the metal \rightarrow ligand charge-transfer (MLCT) state has been shown by Malouf and Ford¹¹ to control the photochemistry. When the MLCT absorption is to the blue of ~ 460 nm (in water), photoexcitation leads to ligand replacement by solvent via population of a lower lying ligand field state. For longer wavelength MLCT absorption the photosolvation yield drops sharply, the MLCT state now falling below the photoactive ligand field state.¹¹ The complex with 4-acetylpyridine ($\lambda_{\text{max}} = 523$ nm) falls in the latter group. Leroi and co-workers¹² have recently shown it possible to obtain the excited-state RR spectrum of this complex but not of the complex with pyridine itself ($\lambda_{\text{max}} = 405$ nm), whose charge-transfer state lies above the ligand field state; the lifetime of the charge-transfer state was presumably too short to permit its RR spectrum to be recorded (although weak enhancement due to the mismatch of the 532-nm laser line with the MLCT transition can also account for the absence of an observable spectrum).

In this study we report RR spectra of $\text{Ru}^{\text{II}}(\text{NH}_3)_5(4,4'\text{-bpy})$ (I) and of $\text{Ru}^{\text{II}}(\text{NH}_3)_5(4,4'\text{-bpyH}^+)$ (IH^+) in its ground and excited states, using 532-nm excitation from a pulsed YAG laser. These complexes show long-wavelength MLCT absorption (480 and 570 nm) and low photoaquation quantum yields.¹³ The excited-state RR frequencies are interpreted as arising from the MLCT state, in which the transferred electron is delocalized over the two bipyridine rings, supporting a quinoid-like resonance structure. In this structure a negative charge is concentrated on the N atom not coordinated to Ru. Consistent with the enhanced basicity expected for this state, the excited-state RR spectrum at pH 7 indicates partial protonation of the complex. Recent picosecond absorption transient measurements by Winkler et al.¹³ have shown short lifetimes for the MLCT states and support a more detailed model of excited-state ordering. The pumping of the excited-state RR spectra despite the short lifetimes is attributable to the high photon flux in the 10-ns YAG pulses and high RR cross sections

- (1) Sutin, N.; Creutz, C. *Adv. Chem. Ser.* **1978**, No. 168, 1.
- (2) Meyer, T. J. *Acc. Chem. Res.* **1978**, *11*, 94.
- (3) Hipps, K. W. *Inorg. Chem.* **1980**, *19*, 1390.
- (4) Felix, F.; Ferguson, J.; Güdel, H. U.; Ludi, A. *J. Am. Chem. Soc.* **1980**, *102*, 4096.
- (5) Dallinger, R. F.; Woodruff, W. H. *J. Am. Chem. Soc.* **1979**, *101*, 4391.
- (6) Bradley, P. G.; Kress, N.; Hornberger, B. A.; Dallinger, R. F.; Woodruff, W. H. *J. Am. Chem. Soc.* **1981**, *103*, 7441.
- (7) Forster, M.; Hester, R. A. *Chem. Phys. Lett.* **1981**, *81*, 42.
- (8) McClanahan, S.; Hayes, T.; Kincaid, J. *J. Am. Chem. Soc.* **1983**, *105*, 4486.
- (9) Smothers, W. K.; Wrighton, M. S. *J. Am. Chem. Soc.* **1983**, *105*, 1067.
- (10) Chung, Y. C.; Leventis, N.; Wagner, P. J.; Leroi, G. E. *J. Am. Chem. Soc.* **1985**, *107*, 1416.
- (11) Malouf, G.; Ford, P. C. *J. Am. Chem. Soc.* **1977**, *99*, 7213.
- (12) Chung, Y. C.; Leventis, N.; Wagner, P. J.; Leroi, G. E. *J. Am. Chem. Soc.* **1985**, *107*, 1414.
- (13) Winkler, J.; Netzel, T. L.; Creutz, C.; Sutin, N. *J. Am. Chem. Soc.*, in press.

* To whom correspondence should be addressed.

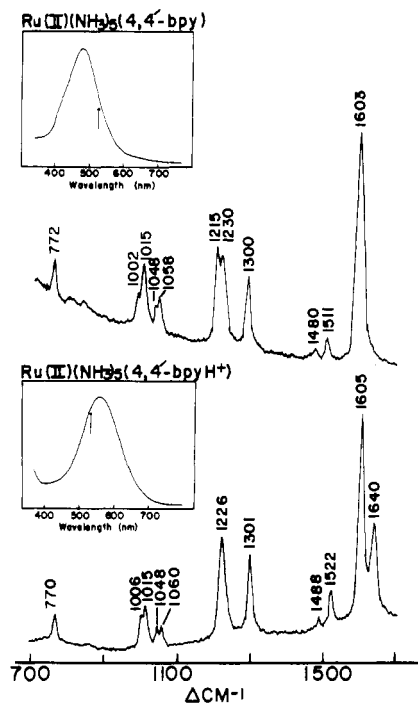


Figure 1. RR spectra of $\text{Ru}^{\text{II}}(\text{NH}_3)_5(4,4'\text{-bpy})$ (top) and $\text{Ru}^{\text{II}}(\text{NH}_3)_5(4,4'\text{-bpyH}^+)$ (bottom) produced with 530.9-nm CW excitation (Kr^+). The inset shows the absorption spectra with the laser wavelength indicated by an arrow. See Experimental Section for details.

for the excited state. The short lifetimes, however, imply very rapid proton transfer to the excited state at pH 7, which is suggested to involve excitation in a strongly H-bonded complex.

Experimental Section

$[\text{Ru}(\text{NH}_3)_5(4,4'\text{-bpy})](\text{PF}_6)_2$ was prepared according to the general procedure of Ford et al.¹⁴ for the synthesis of pentaammineruthenium(II) complexes of aromatic nitrogen heterocycles. Silver trifluoroacetate was prepared from 0.15 g of silver(I) oxide dissolved in 4 mL of trifluoroacetic acid (HTFA). To this was added 0.22 g of chloropentaammineruthenium(III) dichloride (Strem), which after filtration yielded a solution of chloropentaammineruthenium(III) trifluoroacetate. Zinc amalgam was employed to reduce the ruthenium(III) complex in the presence of 2.0 g of 4,4'-bipyridyl hydrate (~ 30 -fold excess) added with an additional 2 mL of HTFA. After filtration, 0.72 g of ammonium hexafluorophosphate was added to the brilliant purple filtrate and the resultant product, pentaamine(4,4'-bipyridine)ruthenium(II) hexafluorophosphate, was washed with absolute ethanol and dry diethyl ether and was air-dried. The absorption spectra obtained from the product dissolved in deionized water displayed $\lambda_{\text{max}} = 480$ nm ($\epsilon = 12600 \text{ M}^{-1} \text{ cm}^{-1}$) for $\text{Ru}^{\text{II}}(\text{NH}_3)_5(4,4'\text{-bpy})$ and $\lambda_{\text{max}} = 570$ nm ($\epsilon = 13800 \text{ M}^{-1} \text{ cm}^{-1}$) for $\text{Ru}^{\text{II}}(\text{NH}_3)_5(4,4'\text{-bpyH}^+)$ (0.1 M HCl). The concentration of the complex for Raman acquisition was typically 1 mM.

The visible excitation source for continuous-wave Raman spectra was the 530.9-nm line of the Kr^+ laser. A Spex 1401 double monochromator was used to disperse and scan the scattered light. Typical laser powers were 100 mW. Data points were collected at 0.5 cm^{-1} increments with $\sim 5 \text{ cm}^{-1}$ resolution for a total of 3 s/point. RR spectra were recorded for frozen aqueous samples mounted on a copper cold finger (77 K) with 135° backscattering geometry.¹⁵

The second harmonic (532 nm) of a pulsed Nd:YAG laser (Quanta-Ray DCR-2A) was employed to both create and probe the excited states of the complex. The resultant pulses were 10 ns in width with a repetition rate of 10 Hz. The laser beam intersected the sample in the free-jet portion (1-mm diameter) of a recirculating flow system containing 3–5 mL of sample.¹⁶ A 120° backscattering geometry was used. The data were collected at 0.33 \AA increments for 3 s/point at $\sim 5\text{-cm}^{-1}$ resolution.

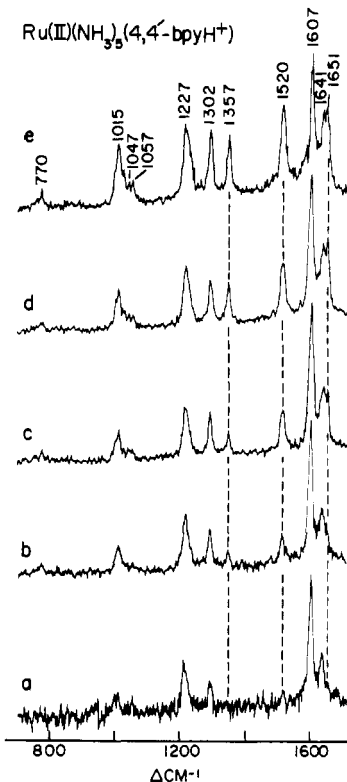


Figure 2. RR spectra of $\text{Ru}^{\text{II}}(\text{NH}_3)_5(4,4'\text{-bpyH}^+)$ produced with 532-nm pulsed excitation (Nd:YAG) with (a) Q switch removed, resulting in 250- μs pulses, and (b–e) Q switch replaced (10-ns pulses) and increasing power levels applied (0.5–3 mJ/pulse). See Experimental Section for details.

The monochromator used to disperse the Raman-scattered light was a 1.26-m Spex single-scanning monochromator. The pulsed output of the photomultiplier tube was processed with a PAR Model 162 boxcar amplifier.

Non-Q-switched radiation (532 nm), resulting in pulse widths of 250 μs , was also used to obtain ground-state spectra of the ruthenium complex for comparison with the CW spectra.

Results

Figure 1 shows RR spectra obtained with 530.9-nm CW laser excitation for I in aqueous solution (pH 12.5—the same spectrum was observed at pH 7 but was slightly less well resolved) and for IH^+ , at pH 1.5; absorption spectra are shown in the inset. Both RR spectra show a strong band at 1605 cm^{-1} , moderate-intensity bands at 1300 and $\sim 1225 \text{ cm}^{-1}$, and weaker bands at ~ 770 , 1006 , 1015 , 1048 , 1060 , 1485 , and 1520 cm^{-1} . The most notable changes between I and IH^+ are the development of a new band at 1640 cm^{-1} and the coalescence of the $1215\text{--}130\text{-cm}^{-1}$ doublet into a single band at 1226 cm^{-1} . The remaining frequencies are shifted only slightly.

Figure 2 shows RR spectra for IH^+ obtained with 532-nm excitation from a pulsed YAG laser, incident on a recirculating sample. The bottom spectrum was obtained with the Q switch removed, resulting in the production of long (250 μs) pulses, which spread out the photons so that only the ground-state spectrum is seen. The features are similar to those seen with 530.9-nm CW laser excitation (Figure 1), although the signal/noise is inferior and the weak peaks cannot be seen. The remaining spectra were obtained at increasing power levels with the Q switch in, giving 10-ns pulses. The signal/noise improves, and three new peaks appear as the laser power increases, at 1651 , 1520 , and 1357 cm^{-1} . (The 1520-cm^{-1} band grows on top of a small peak present in the ground-state spectrum, Figure 1.) These are assigned to Raman modes of the excited state. The power dependence is reversible, and at the end of the experiment no significant change was observed for the absorption spectrum. (The photoaquation quantum yield for NH_3 replacement is $(4 \pm 3) \times 10^{-3}$.¹³ However, 2-photon events corresponding to excitation in the MLCT state have been

(14) Ford, P.; Rudd, D. F. P.; Gaunder, R.; Taube, H. *J. Am. Chem. Soc.* **1968**, *90*, 1187.

(15) Czernuszewicz, R. S.; Johnson, M. K. *Appl. Spectrosc.* **1983**, *37*, 297.

(16) Fodor, S. P. A.; Rava, R. P.; Copeland, R. A.; Spiro, T. G. *J. Raman Spectrosc.*, in press.

Table I. Comparison of Ground- and Excited-State RR Frequencies (cm^{-1}) for $\text{Ru}^{\text{II}}(2,2'\text{-bpy})_3$ and $\text{Ru}^{\text{II}}(\text{NH}_3)_5(4,4'\text{-bpy})$ (I) and Correlations with Biphenyl

symm	ν	RR frequencies							biphenyl radical anion ^c
		biphenyl ^a	$\text{Ru}(\text{bpy})_3^{2+}$ ^b	$\text{Ru}(\text{bpy})_3^{2+*}$ ^b	I	I*	IH ⁺	IH ⁺⁺	
A _g	4	1612	1605	1545	1603	1506	1605	1520	1587
B _{3u}	4	1597			<i>d</i>	1636	1640	1651	
B _{2u}	3	1570	1560	1499					
A _g	5	1507	1489	1477	1511		1522		1493
B _{3u}	5	1482			1480		1480		
B _{2u}	4	1432	1448	1425					
B _{2u}	5	1383							
A _g	6	1285	1317	1363	1300	1339	1301	1357	1326
B _{2u}	6	1272	1264 ^e	1283					
A _g	7	1190	1173	1211	1230		1226		
B _{3u}	6	1176			1215		1226		
B _{2u}	7	1156	1109	1098					
B _{2u}	8	1074	1067						
B _{3u}	7	1040			1058		1060		
A _g	8	1030	1041	1030	1048		1048		1017
B _{3u}	8	1008			1002		1006		
A _g	9	1003	1027	1012	1015		1015		979
B _{3u}	9	965							
A _g	10	742	766	741	772		770		721
B _{2u}	9	628	663						
B _{3u}	10	609							
A _g	11	315							

^a From ref 17. ^b Data from ref 7; the less complete frequency list from ref 6 is in agreement. ^c From ref 19. ^d Probably overlapped with A_g (4). ^e Appears to contain two bands, at 1276 and 1254 cm^{-1} , when excited at 350.6 nm.^{6,7}

shown to produce a 10% quantum yield for NH₃ replacement when picosecond pulses were used.¹³ The nanosecond laser pulses in this experiment are likely to produce NH₃ quantum yields between these two limits. Importantly, partial replacement of NH₃ ligands with H₂O is not expected to alter either the absorption¹¹ or the RR spectrum appreciably.)

Figure 3 shows the same experiment for I, at pH 7. Again three new features grow in with increasing laser power, but in this case they appear to be doubled. This is seen most clearly for the pair of bands at 1636/1651 cm^{-1} . The higher of these frequencies is the same as that observed for the protonated complex. Likewise the other two features are broad and appear to contain pairs of bands, one located at the frequency shown by the protonated complex and the other at a slightly lower frequency. We interpret this as reflecting the superposition of two spectra, one from protonated species, formed by proton transfer in the excited state, and the other from unprotonated species, whose frequencies are 15–20 cm^{-1} lower. Again, there was no detectable change in the ground-state RR or absorption spectra after the Raman experiments.

Discussion

Normal Modes and Excited-State Structure: Comparison with $\text{Ru}(\text{bpy})_3^{2+}$. In this section we consider the assignment of the RR bands of the 4,4'-bipyridine complex in its ground and excited state. This is best done in connection with spectral assignments for $\text{Ru}(\text{bpy})_3^{2+}$, for which more complete data are available.^{6,7} Although $\text{Ru}(\text{bpy})_3^{2+}$ has been thoroughly studied with respect to the nature of its ground and excited state RR spectra, band assignments do not appear to have been made.

We propose to assign the spectra of both $\text{Ru}(\text{bpy})_3^{2+}$ and I with reference to the normal modes of biphenyl, which have been analyzed in detail by Zerbi and Sandroni.¹⁷ Biphenyl is similar to the bipyridines in its molecular and electronic structure but has higher symmetry. Assuming a D_{2h} (planar) average structure, the in-plane biphenyl modes are classified as A_g (totally symmetric), B_{1g}, B_{2u}, and B_{3u}; the B_{2u} and B_{3u} modes are *x* and *y* polarized, where *y* is the direction of the inter-ring bond. When Ru coordinates to either 4,4'-bipyridine or 2,2'-bipyridine, the local symmetry is C_{2v} (see Figure 4); the C₂ axis is *y* for 4,4'-bipyridine but *x* for 2,2'-bipyridine. When the biphenyl modes are correlated,

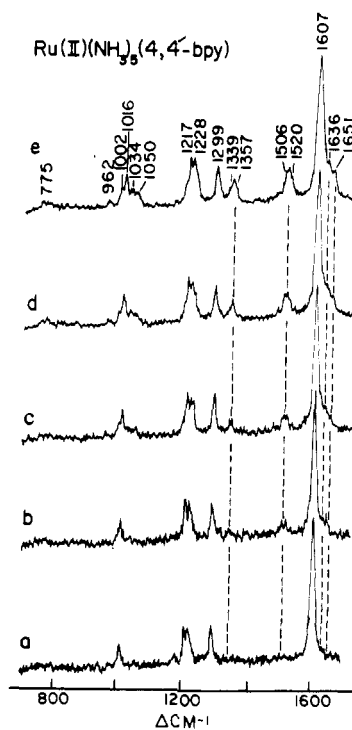


Figure 3. RR spectra of $\text{Ru}^{\text{II}}(\text{NH}_3)_5(4,4'\text{-bpy})$ produced with 532-nm pulsed excitation (Nd:YAG) with (a) Q switch removed, resulting in 250- μs pulses, and (b-e) Q switch replaced (10-ns pulses) and increasing power levels applied (0.5–3 mJ/pulse). See experimental Section for details.

the A_g modes remain totally symmetric (A₁) for both bipyridines, while the B_{3u} modes correlate with A₁ for 4,4'-bipyridine, and the B_{2u} modes correlate with A₁ for 2,2'-bipyridine.

Enhancement of bipyridine Raman bands via resonance with the MLCT transitions is expected for totally symmetric modes (A₁) along whose coordinates the excited-state potential is displaced. Consequently, bands correlating with the biphenyl A_g modes are expected in RR spectra of both I and $\text{Ru}(\text{bpy})_3^{2+}$, while B_{3u}-derived and B_{2u}-derived modes are expected to be activated for I and for $\text{Ru}(\text{bpy})_3^{2+}$, respectively. IH⁺ has the same symmetry

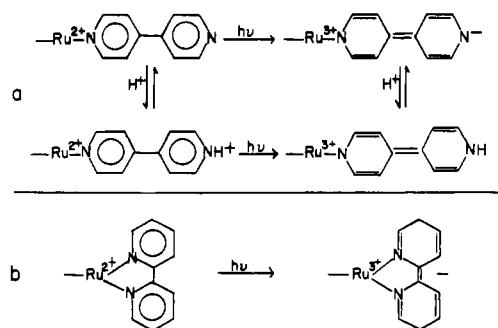


Figure 4. Structural diagrams of species discussed in this study: (a) $-\text{Ru}-(4,4'\text{-bpy})$ and $-\text{Ru}-(4,4'\text{-bpyH}^+)$; (b) $-\text{Ru}-(2,2'\text{-bpy})$. The diagrams show suggested dominant resonance forms for the photoexcited MLCT states.

as I and a similar enhancement pattern is anticipated, although the bands may be shifted in frequency. With these considerations, the observed RR bands of I, IH^+ , and $\text{Ru}(\text{bpy})_3^{2+}$ are readily correlated with the biphenyl vibrations, as shown in Table I. Here all of the A_g , B_{2u} , and B_{3u} biphenyl modes¹⁷ are listed, excepting the C-H stretching modes, three in each symmetry block, which occur near 3000 cm^{-1} and are not expected to be resonance enhanced in the Ru complexes.

Correlations for I and IH^+ are aided by the fact that 10 of the biphenyl modes occur in A_g/B_{3u} pairs that are nearby in frequency (see Table I) because they are symmetric and antisymmetric (with respect to the inter-ring bond) combinations of modes that are localized on the individual phenyl rings.¹⁷ The relatively weak coupling for these modes gives rise to the characteristic doublet pattern for several bands of the I and IH^+ spectra (Figure 1). In each of these cases $\text{Ru}(\text{bpy})_3^{2+}$ shows only a single band, due to the absence of B_{3u} mode activation, but additional bands fall between the I doublets, which are the B_{2u} -derived modes. Table I shows that every biphenyl mode can be accounted for in this way, with the exception of B_{2u} mode 5 at 1383 cm^{-1} and B_{3u} mode 9 at 965 cm^{-1} , which apparently lack sufficient enhancement for detection in the appropriate bipyridine spectra. B_{3u} mode 10 (609 cm^{-1}) and A_g mode 11 (315 cm^{-1}) are below the RR spectral cutoffs. There are no exceptions to the symmetry rules; A_g modes appear in all spectra, but B_{2u} modes are seen only for $\text{Ru}(\text{bpy})_3^{2+}$, and B_{3u} modes are seen only for I and IH^+ . The success of the correlations lends considerable confidence to the assignment scheme.

The frequencies of corresponding modes between biphenyl and the coordinated bipyridines are surprisingly close. None of the differences exceed 40 cm^{-1} , and most are within 20 cm^{-1} . Protonation of I produces several frequency shifts attributable to polarization effects. The most dramatic manifestation is the appearance of a new band at 1640 cm^{-1} . This is attributed to an upshift of the B_{3u} -derived mode (4) expected at ~ 1600 cm^{-1} (1597 cm^{-1} in biphenyl) in I, which is evidently overlapped with the A_g -derived mode (4) at 1603 cm^{-1} . A similar upshift, 1583 \rightarrow 1630 cm^{-1} , is seen for the ν_{8a} mode of pyridine itself upon protonation.¹⁸ In effect, protonation of I can be seen as uncoupling the two biphenyl-related modes 4, A_g and B_{3u} , localizing them on the inner and outer (with respect to Ru) pyridine rings.

Table I also gives suggested assignments of the excited state RR bands of all three complexes, $\text{Ru}(\text{bpy})_3^{2+}$, I^* , and IH^* . The correlations are less meaningful than for the ground states because appreciable changes in the normal mode compositions are expected upon charge-transfer excitation. As indicated in Figure 4, the CT state is expected to have significant contributions from quinonoid resonance structures of the bipyridyl anions; the altered bond orders are expected to affect the normal modes appreciably. Nevertheless the excited-state frequencies fall into a reasonable relationship with the ground-state frequencies, giving plausible

correlations. The mode frequencies for biphenyl anion¹⁹ provide a useful guide.

The most interesting effect is the large upshift, 40–50 cm^{-1} , in the A_g mode (6) frequency near 1300 cm^{-1} . This shift is seen upon exciting all three Ru complexes and also upon reducing biphenyl to the anion. This mode has a large contribution from the inter-ring C–C bond.¹⁷ (It is for this reason that there is no B_{3u} counterpart (Table I), B_{3u} modes being antisymmetric with respect to the inter-ring bond.) The quinonoid contribution to the excited-state structure implies an increase in the inter-ring bond order, nicely accounting for the frequency upshift. A similar interpretation for the biphenyl anion by Yamaguchi et al.¹⁹ was supported by the results of molecular orbital calculations.

Two nearby $\text{Ru}(\text{bpy})_3^{2+}$ modes, B_{2u} (6) and A_g (7), also shift up on excitation, while the remaining modes shift down, as they do in the biphenyl anion. Excited-state data are much less complete for I^* and IH^{*+} than for $\text{Ru}(\text{bpy})_3^{2+}$, because of their much shorter lifetimes. Even at the highest laser power levels available, conversion to the excited state is partial. Aside from the upshifted A_g (6) mode discussed in the preceding paragraph, only two other bands can confidently be attributed to this state. One of these, 1520 cm^{-1} for IH^{*+} and 1506 cm^{-1} for I^* , is assigned to A_g (4) by analogy with the 1587- cm^{-1} band of biphenyl anion and the 1545- cm^{-1} band of $\text{Ru}(\text{bpy})_3^{2+}$. The downshift relative to biphenyl or the Ru complex ground states increases in the order biphenyl(1-) < $\text{Ru}(\text{bpy})_3^{2+}$ < IH^{*+} < I^* , perhaps reflecting the increasingly dipolar character of the structures (see Figure 4). The highest frequency I^* and IH^{*+} bands, 1636 and 1651 cm^{-1} , have no correspondence in the spectra of $\text{Ru}(\text{bpy})_3^{2+}$ or biphenyl(1-). They are therefore assigned to the B_{3u} (4) mode, which does not appear in the latter spectra. The upshift of this mode in the excited state must reflect altered coupling across the inter-ring bond, perhaps associated with its increased bond order.

Excited-State Dynamics and Protonation. For $\text{Ru}(\text{bpy})_3^{2+}$ the excited state is relatively long-lived (~ 1 μs),¹ and 10-ns YAG laser pulses can readily deplete the ground state.^{5,6} For I, however, the excited-state lifetime has recently been determined by Winkler et al.¹³ to be much shorter. At pH 7, two absorption transients were seen, with lifetimes of 36 and 230 ps, while at pH 1, the lifetime was less than the instrument resolution, ~ 30 ps. At first sight it is surprising that any excited-state signal can be detected with 10-ns laser pulses. The pumping rate can, however, be sufficient to maintain an appreciable fraction of the molecules in the excited state during the pulse. For lifetimes much shorter than the pulse length, the steady-state excited-state fraction is given²² by $C^*/C_0 = k_1/(k_1 + k_d)$, where k_d is the excited-state decay rate and k_1 is the pumping rate: $k_1 = \phi^*(2.3 \times 10^3)\epsilon I_0$ where ϕ^* is the quantum yield for excited-state formation, ϵ is the ground-state molar absorptivity at the excitation wavelength, and I_0 is the incident photon intensity (einstein $\text{cm}^{-2} \text{s}^{-1}$). For the 10-ns YAG laser pulses at 532 nm where the molar absorptivity of I (pH 7) is 7900 $\text{M}^{-1} \text{cm}^{-1}$, $C^*/C_0 \sim 0.5$ or 0.8 for excited-state lifetimes of 36 or 230 ps, when the pulse energy is ~ 3 mJ, the maximum value used in these experiments, and the focused laser spot is assumed to be ~ 0.1 mm in radius (ϕ^* is assumed to be 1). This calculation shows that an appreciable steady-state concentration of I^* can be achieved under reasonable pulsed laser conditions. The C^*/C_0 ratio at pH 1.5 would be smaller than this since the excited-state lifetime is shorter.

The excited-state fraction is not easily estimated from the RR spectra, since the resonance enhancement factors are unknown. The transient absorption spectra show relatively small changes with respect to the ground-state spectra,¹³ establishing that the excited states absorb strongly at the laser wavelength, and strong resonance enhancement is therefore expected. At pH 7, small absorption increases are seen in the 550-nm region, while at pH

(18) Dollish, F. R.; Fateley, W. G.; Bentley, F. F. *Characteristic Raman Frequencies of Organic Compounds*; Wiley: New York, 1974; p 264.

(19) Yamaguchi, S.; Yoshimisu, N.; Maeda, S. *J. Phys. Chem.* **1978**, *82*, 1078.

(20) Streckas, T. C.; Mandal, S. K. *J. Raman Spectrosc.* **1984**, *15*, 109.

(21) Strukl, J. S.; Walter, J. L. *Spectrochim. Acta, Part A* **1971**, *27A*, 223.

(22) Creutz, C.; Chu, M.; Netzel, T. L.; Okimura, M.; Sutin, N. *J. Am. Chem. Soc.* **1980**, *102*, 1309.

1, the difference spectrum at zero delay indicates a blue shift in the absorption spectrum relative to the ground state.¹³ This would bring the laser wavelength into better resonance with the absorption maximum, an effect that might account for the stronger signal seen for the excited-state bands at pH 1.5 (Figure 2) despite the shorter lifetime of the protonated excited state.

The observation that the excited-state RR bands at pH 7 are superpositions of two spectra, one of which shows frequencies that are the same as are observed at pH 1.5, implies that some of the excited-state molecules are protonated even at pH 7. Certainly the excited state is expected to be more basic than the ground state, since protonation neutralizes the charge produced at the terminal N atom in the excited state (Figure 4). This stabilization is reflected in the red shift of the absorption maximum from 480 nm at pH 7 to 570 nm at pH 1.5. This wavelength shift can be used to estimate the excited-state pK_a shift²³

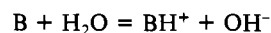
$$\Delta(pK) = 0.00209(\bar{\nu}_B - \bar{\nu}_{BH^+})/\text{cm}^{-1}$$

via the Förster cycle,²⁴ in which the difference in the ground- and excited-state protonation free energies is assumed to be given by the difference in the S_1-S_0 energy gaps for the protonated and unprotonated forms. (The assumption in this equation that the difference in the 0-0 energies is given by the difference in the absorption maxima introduces a significant uncertainty.²³) For I and IH^+ the absorption frequency difference is 3300 cm^{-1} , giving an estimated $\Delta(pK_a)$ of 6.9. When added to the pK_a of the ground state, 4.5,¹³ this gives an excited-state pK_a of 11.4. Thus essentially all of the excited molecules are expected to be protonated at equilibrium.

It is unclear, however, what fraction of the molecules become protonated within the very short lifetimes of the excited states.

(23) Ireland, J. F.; Wyatt, P. A. H. *Adv. Phys. Org. Chem.* 1976, 12, 135.
 (24) Förster, T. Z. *Elektrochem.* 1950, 54, 531.

At equilibrium, the ratio of the forward, k_f , and reverse, k_r , rate constants for the protonation reaction



must give the equilibrium constant

$$K_B = 10^{-14}/10^{-11.4} = 10^{-3.6} = k_f/k_r$$

The maximum value of k_r is the diffusion-controlled rate constant $\sim 10^{10}\text{ M}^{-1}\text{ s}^{-1}$, and consequently the maximum value of $k_f = \sim 10^{10}K_B = 10^{6.4}\text{ s}^{-1}$. With this rate constant, less than 0.1% of the initially excited molecules are expected to be protonated within even the longer of the two pH 7 lifetimes, 230 ps. Equilibrium conditions, however, are not expected to apply to the initially excited species, since the solvent cage is that appropriate for the ground state. It is likely that some of the excited molecules find themselves with H-bonded water molecules that are well positioned for proton transfer. Other examples of very fast excited-state proton-transfer reactions have been noted. For example, in a study of 2-naphthol fluorescence decay, Ofran and Feitelson²⁵ were forced to assume that some of the naphthol was deprotonated in the initially excited S_1 state in order to explain their data. Heterogeneity is evident in the excited I population at pH 7 from the finding of two lifetimes, both of which are attributable to the charge-transfer state.¹³ It is possible that the fraction with the short lifetime, 36 ps, is made up of those molecules that have undergone nonequilibrium proton transfer or else are sufficiently strongly H-bonded to have the same RR frequencies as protonated molecules.

Acknowledgment. We thank Dr. Thomas Netzel for suggesting this problem to us and for communicating the results of his work prior to publication. This work was supported by Grant AC02-81ER10861 from the U.S. Department of Energy.

(25) Ofran, M.; Feitelson, J. *Chem. Phys. Lett.* 1973, 19, 427.

Contribution from the Polymers Technology Group, Chemical Technology Center, Exxon Chemical Company, Baytown, Texas 77522, and Chemistry Department, University of Edinburgh, Edinburgh, Scotland

X-ray Photoelectron Spectra of Mixed-Valence Diruthenium Complexes. Distinguishing between Strongly and Weakly Interacting Metals in Delocalized Class III Complexes

Patrick Brant* and T. Anthony Stephenson†

Received July 30, 1986

X-ray photoelectron (XP) spectra have been recorded for a series of trichloro-bridged diruthenium complexes containing the $[\text{RuCl}_3\text{Ru}]^{n+}$ ($n = 1-3$) fragment. Along with symmetrical and asymmetrical $[\text{Ru(II),Ru(II)}$] and $[\text{Ru(III),Ru(III)}$] complexes, the series contains both asymmetrical, mixed-valence class II complexes and a symmetrical, mixed-valence class III complex, $[\text{As}(p\text{-tol})_3]_2\text{ClRuCl}_3\text{RuCl}[\text{As}(p\text{-tol})_3]_2$ (**7**; $p\text{-tol} = p\text{-tolyl}$). Symmetrical $[\text{Ru(II),Ru(II)}$] and $[\text{Ru(III),Ru(III)}$] complexes give single Ru $3d_{5/2}$ peaks in accord with the chemically identical environments of the two ruthenium ions. Either one or two Ru $3d_{5/2}$ photolines are observed in spectra of asymmetrical $[\text{Ru(II),Ru(II)}$] complexes depending on just how dissimilar are the ruthenium local environments. The trapped-valence, asymmetrical $[\text{Ru(II),Ru(III)}$] complexes also yield one or two Ru $3d_{5/2}$ lines in their spectra, but in any case the lines are broader than the single Ru $3d_{5/2}$ line (full width at half-maximum 1.3 eV) observed for the symmetrical, average valence complex **7**. This result contrasts with previous XP spectra of Creutz-Taube-type class III complexes. Spectra of these complexes yielded two Ru $3d_{5/2}$ photoionization states of equal intensity split by 3.4-3.6 eV. In the Creutz-Taube-type complexes the unpaired electron originally equally shared between ruthenium centers in the ground state is stated to become localized on one or the other ruthenium under the influence of the Ru 3d core hole during photoemission. The absence of such splitting of the Ru $3d_{5/2}$ (and Ru $3p_{3/2}$) lines in the XP spectrum of **7** is consistent with much stronger electronic coupling between the two metal centers in this complex. It is estimated that whereas Creutz-Taube complexes have an electronic exchange parameter, α' , of 0.10 or less, this parameter must be greater than 0.9 for complex **7**.

Introduction

Over the past few years substantial effort has been expended¹⁻¹¹ assessing the degree of electron delocalization in mixed-valence dimetal complexes of general formula M^2M^{2+1} . Various spec-

troscopic measurements have been used to assign complexes to Robin and Day's¹² II (trapped valence) and III (average valence)

- (1) Creutz, C.; Taube, H. *J. Am. Chem. Soc.* 1969, 91, 3988.
- (2) Meyer, T. J. *Acc. Chem. Res.* 1978, 11, 94.
- (3) Bunker, B. C.; Drago, R. S.; Hendrickson, D. N.; Richman, R. M.; Kessell, S. L. *J. Am. Chem. Soc.* 1978, 100, 3805.
- (4) Allen, G. C.; Green, M.; Lee, B. J.; Kirsch, H. P.; Stone, F. G. A. *J. Chem. Soc., Chem. Commun.* 1976, 794.

* To whom all correspondence should be addressed at Exxon Chemical Co.
 † Deceased.